Gravity Driven Flow of Particle-Laden Thin Films

Wylie Rosenthal, Spencer Hill, Paul Latterman, Paul David

August 5, 2011

1 Introduction

1.1 Applications

Flow of particle-laden fluid may be observed in nature and is applicable to many problems in science, engineering and industry. Mud slides, erosion and turbidity currents may be modeled using equations derived from experiments with particle-laden liquid. Current industrial processes including paper making, food characterization, and the application of fertilizers all require a knowledge of the dynamics of particle-laden fluid.[1]

1.2 Previous Work

1.2.1 Huppert

Herbert E. Huppert produced an accurate model for fluid flow velocity and front wavelength[2]. A fluid's position on the ramp is predicted to be directly proportional to $t^{\frac{1}{3}}$. This model relies on the lubrication theory[3] and the approximations underlying it. Huppert predicts that the position of the front, x, is less than $x_N = (9A^{\frac{1}{2}}gsin\alpha/4\nu)^{\frac{1}{3}}t^{\frac{1}{3}}$ (eqn. 9) derived below.

The momentum equation for a fluid moving down an incline plane is given by

$$0 = g\sin\alpha + \nu u_{zz} \tag{1}$$

when ignoring the surface tension and contact line effects. The momentum of the fluid is dependent on the incline angle α, the fluids dynamic viscosity coefficient ν, and shear acceleration u_{zz}. Using conservation laws for volume

[1] B. P. Cook, Theory for particle settling and shear-induced migration in thin-film liquid flow, Phys. Rev. E 78 (2008) 045303.

[2] Huppert, "Flow and instability of a viscous current down a slope", Nature 1982

[3] Batchelor, G. K. *An introduction to fluid Dynamics*,Cambridge University Press

and momentum a nonlinear partial differential equation for the height of the fluid is written

$$0 = h_t + (g\sin(\alpha/\nu))h^2 h_x \tag{2}$$

or equivalently

$$h(x,t) = (-\frac{h_t}{H_x g}\csc(\alpha/\nu))^{1/2} \tag{3}$$

This equation leads to a continuity equation calculating the cross sectional area A of the fluid

$$A = \int_0^{x_N(t)} H(x,t)dx \tag{4}$$

The limits of integration go from the starting position x to the current position, $x_n(t)$, the position at a given time. By rearranging equation 2 the velocity of the fluid can be determined

$$\frac{dx}{dt} = (g\sin(\alpha/\nu))h^2 \tag{5}$$

Given an initial height, $h(x,0) = f(x)$, and initial position, x_0, the position of the flow is given as

$$x = x_0 + (g\sin(\alpha/\nu))f(x)^2(x_0)t. \tag{6}$$

Equation 2 thus has a solution

$$h = [\frac{1}{t}\frac{\nu(x-x_0)}{g\sin\alpha}]^{1/2} \tag{7}$$

At the limit $x_0 << x$ equation 7 becomes

$$h \to [\frac{1}{t}\frac{\nu x}{g\sin\alpha}]^{1/2}. \tag{8}$$

Equation 8, in conjunction with equation 4, produces a means of evaluating the length of the current

$$0 \leq x \leq x_N = (9A^{\frac{1}{2}}gsin\alpha/4\nu)^{\frac{1}{3}}t^{\frac{1}{3}} \tag{9}$$

This may be written as a simple proportionality equation be combining the fluid dependent constant as $\hat{C_N} = \hat{t}/\hat{x_N}^{\frac{1}{3}}$

$$\hat{x_N} = (\frac{\hat{t}}{\hat{C_N}})^{1/3} \tag{10}$$

At x_n the profile of the current ends with the height of $h_n(t) = 1.5A/x_n$. The solution may be smoothed by including higher order terms to account for the effects of surface tension.

1.2.2 Ward

An experimental study of fixed-volume particle-laden flow down an inclined plane similar to our experimental setup was preformed by Ward et al. This paper presented the results of experimental tests of Huppert's model for particle-laden slurries. Huppert's final equation (9) is non-dimensionalized and made to explicitly include particles in the fluid, thereby giving the equation

$$C_N = \frac{9\rho(\bar{\phi})A^2 g\hat{C_N} sin\alpha}{4\mu_L} \tag{11}$$

where $\bar{\rho}(\phi)$ is the average density of the slurry, A is is the cross sectional area defined as volume divided by track width w ($A = V_T/w$) and absolute viscosity is μ_L. Ward examined flows of particles that had a density one-tenth that of the fluid, and heavier particles with densities two and a half times that of the fluid. The experimentation of the average front position with particles differed from Huppert's work with pure liquid. Particles were found to change the geometry of the front of the fluid. This change in the stability of the front is observed and changes the wavelength, resulting in hindered fingering as the concentration of particles,ϕ, increases. Despite the particle's effect on the geometry of the front, the average position, x_n, is determined to be comparable to that predicted by Huppert's model. An experimentally important characteristic found by Ward is the initial transient period where the fluid and particles have a higher velocity than predicted. The duration of this period increases with increasing concentration for the higher density particles, but was found to be independent of concentration for the lower density particles as seen in Figure 1 and Figure 2. After this transient period flow becomes well-developed and behaves according to Huppert's model.

Of particular interest is Ward's work on particles with a lower density than the mixing fluid. Ward experimented with particles of density $0.15g/cm^3$ in a fluid ten times as dense. Our work primarily focused on particles of densities approximately the same as the fluid up to particles that are half as dense as the fluid. Ward found that the lighter particles moved upward leaving a fluid rich region below, so that the contact with the track is dominated by the fluid. Possibly because the primary contact of the slurry with the track was with liquid, Ward found many similarities between how the pure liquid functions on an incline plane and the light particle mixture. The liquid rich layer below was found to flow down the track by itself and generally highly pronounced fingering was observed. The lighter particles decrease the velocity of the propagating front. This effect increases with the concentration, as the ratio of light particles increase the greater the buoyancy force opposing gravity driven flow slowing the total flow. Despite the differences Ward found the graphs of front position verses $t^{\frac{1}{3}}$ produces a linear relationship

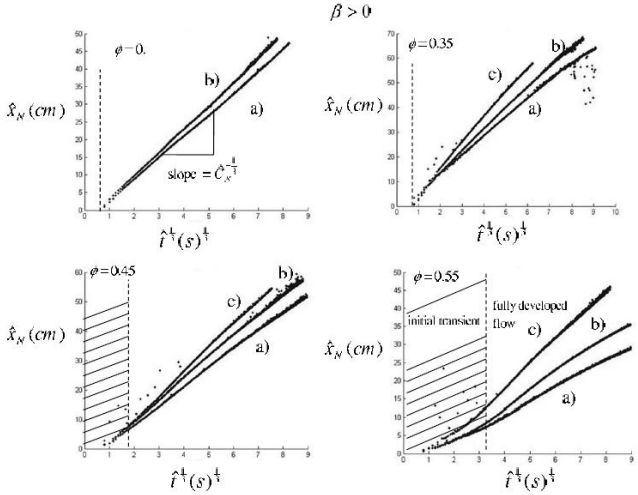

Figure 1: (Taken from Ward et al.) Average front position x_N vs. $t^{1/3}$ for 250 – 425 μm, 0.0214 dynes glass bead slurry mixture. The tilt angles are (a) 35°, (b) 45°, and (c) 55°. These data were used to measure the slopes which contain information for proportionality constant C_N. Note that we do not expect the data to collapse onto one line; rather we expect to see a linear relationship between x_N and $t^{1/3}$ after the initial transients have decayed. The variation at each concentration is due to the difference in inclination angle and/or volume for each experiment. The vertical dashed line roughly indicates the transition from transient to fully developed flow. There are no lines drawn through the data point and no fitting parameters.

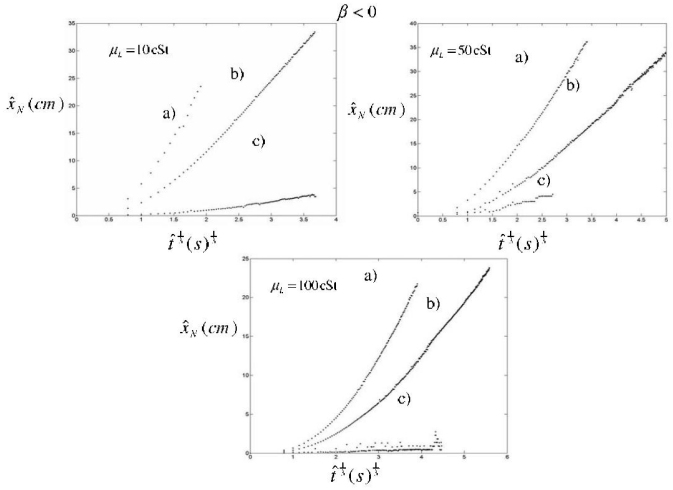

Figure 2: (Taken from Ward et al.) Average front position $x_N$vs $t^{1/3}$ for a buoyant glass sphere slurry mixture with $-3.5x10^{-6}$ dynes particles. The tilt angle is 45°, and concentrations (a) 0.35, (b) 0.45, and (c) 0.55 are shown. Note the transient period is independent of concentration. There are no lines drawn through the data point and no fitting parameters.

between x_N and $t^{1/3}$ after the initial transients have decayed, confirming Huppert's model.

1.3 Overview/Our work

Our work focused entirely on particles that had lesser and comparable densities to that of the surrounding fluid. We aimed at confirming the validity of previous models, originally derived for dense glass particles, for buoyant foamed glass spheres. Extensive experimental studies on three different particle densities revealed that suspensions adhere to only one behavioral regime, particle-rich ridging. The other two regimes observed in heavier particles, settled and well-mixed, were suppressed in lighter particle suspensions.

Analysis of this behavior was done using both experimental and numerical methods. We focused heavily on an extensive comparison to Huppert's front position dynamics for clear fluid as well as experiments on heavy and significantly lighter particle suspensions by Ward et al. Huppert's equation for front position was also tested against a reduced dynamic model proposed in Cook et al for a constant volume thin-fluid film. While both experimental and empirical evaluations of the front dynamics showed different trends, they both deviate from Huppert's original model. We postulate that particle

concentration has a strong affect on the time-dependence of the fluid film front, but further investigation is needed. Another model we used was a steady-state shear model proposed by Murisic et al, which successfully predicted particle concentration along the height of a thin film.

In addition to the stated analyses, we attempted to experimentally verify the hindered settling function first proposed by Richardson and Zaki[4]. We aimed to pictorially use centroid tracking to trace the average particle position of an initially well-mixed suspension with time. Our approach however was unsuccessful and we attribute this to a faulty data-acquisition method.

2 Experimental Setup

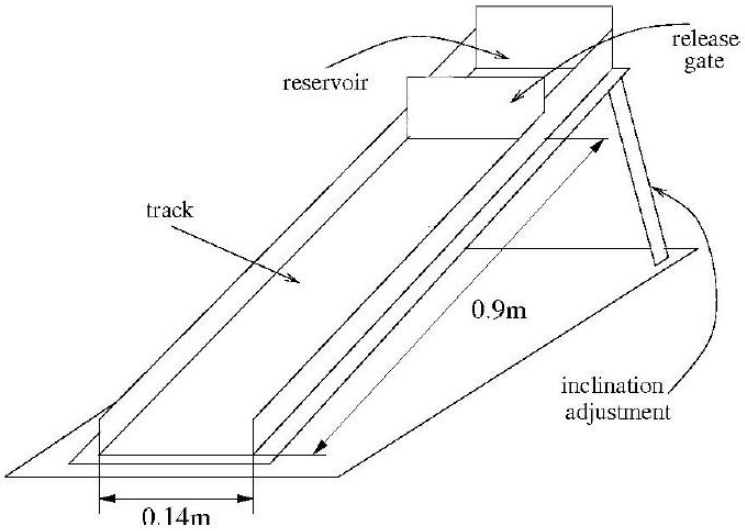

Figure 3: Experimental apparatus with adjustable incline

Figure 3 shows the experimental apparatus we use to conduct our experiments. It consists of an acrylic track with adjustable inclination angle, α, which has a range of 5° - 80°. The track is 0.90m long and 0.14m wide, with 0.02m side walls. A liquid and particle mixture prepared beforehand is poured into the reservoir situated at the top of the track (reservoir dimensions: height × width × length = 0.04 × 0.14 × 0.10m) and the gate is lifted, allowing the mixture to flow down the track, with the contact line initially

[4]Richardson, Zaki, "The sedimentation of a suspension of uniform spheres under conditions for viscous flow", Chemical Engineering Science, 1954

straight. Here, we only focus on experiments with finite, constant suspension volume. The evolution of the flow is monitored using a digital camera, which is positioned above the track and captures images of the moving front at predetermined time intervals, typically once every 1 - 20s depending on the speed of the flow. Using this setup, we are able to monitor the film's motion, starting from release, until the front has reached approximately 0.6m down the track. Images are subsequently analyzed, and each experimental run is classified quantitatively by ridge height, the number of fingers, and the local particle concentrations.

Our experiments involve three different particles, which are foamed glass beads, (Agsco) mixed into silicon oil (Clearco Products). The properties of the particles, which vary in density and diameter, are summarized in Table 1. The values represented are average densities and average sizes since the particles are polydisperse. The silicon oil used is polydimethylsiloxane (PDMS) with a kinematic viscosity of 1000cSt. The particles we use are buoyant and light, i.e. $\rho_p < \rho_l$, where ρ_p and ρ_l are particle and liquid densities respectively.

Table 1: Particle Specifications

Particle	average $\rho(g/cm^3)$	average d (mm)
P1	0.46	0.750
P2	0.64	0.375
P3	1.10	0.200

Suspensions are prepared by first weighing the particles and PDMS individually, pouring PDMS into a container, and then adding particles; slow manual stirring is used until uniform mixture is obtained. Here, the mixtures we focus on have a volume between 66 and 95mL.

The track, gate, and reservoir are cleaned after each experimental run using a squeegee to remove the excess particulate and dust which may accumulate. Although this cleaning procedure does not remove PDMS entirely, it ensures reproducibility of our experimental results.

We carry out a methodical study of the effects of varying inclination angle, particle concentration, and particle size/density. The parameters used in each experiment greatly effect the particle movement within fluid. For each of the three different particles, P1 P2 and P3, we vary the initial particle concentration, ϕ_0, between 0.20 and 0.50, and α between 10° - 50°.

Figure 4: Suspension of glass beads in PDMS fluid

Using Firei software and the digital camera positioned in front of the track, we are able to record still frames of the suspension as it progresses down the incline. This is critical in the front tracking process. Each image includes a time stamp, which allows us to know the time elapsed since the beginning of the run. By creating a user friendly GUI, we semi-automated a method for processing each runs' series of images.

Running the MATLAB GUI allows the user to crop the image such that the focus is only the front of the flow. We programmed a method to convert the image to grayscale and then to a black and white binary image. The program then detects edges using the trace boundary function to outline the front of the flow. This stores the data as a vector of pixel positions. These positions are then averaged to tell the user how far along the incline the average fluid front is. This is the green line shown in Figure 5. The user inputs the time and position, which are stored as pairs in a matrix. This information is then used to create a position vs. time plot and a log-log plot of the same data (shown below in Figure 6). We analyze the results and compare them to expected results from theory.

3 Experimental Results

Data acquired from the front tracking GUI allows us to plot both the position vs. time and log(position) vs. log(time). With a linear, best-fit line, the latter provides us with information about the exponential dependence of position on time. Huppert predicted a $t^{1/3}$ dependence for clear fluid; here, we examine the same dependence but with particle-laden flows instead of clear fluid.

As one can see, the higher the concentration of particles within the fluid,

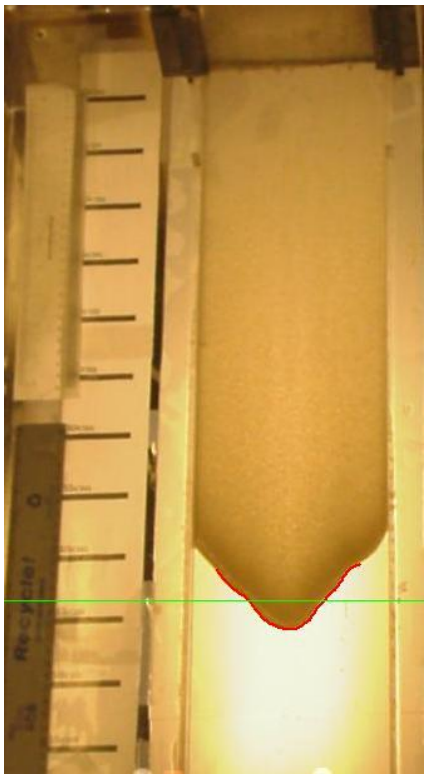

Figure 5: The red line is the front detected by the program after cropping the image; the green one is the calculated average front position

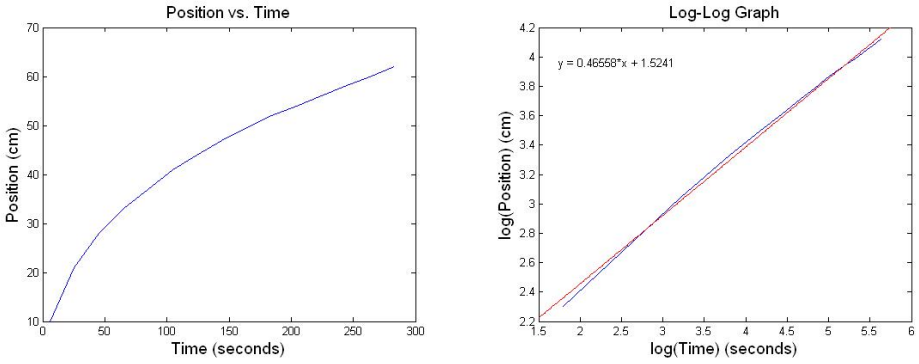

(a) position vs. time

(b) log log plot

Figure 6: 1.10 density, 0.25 Concentration, 30 Degrees

the greater the exponential dependence. This holds true for both particle densities shown. At 0.40 concentration, the particles of $0.64 g/cm^3$ have an exponential dependence of 0.55 and the particles of $1.10 g/cm^3$ show depen-

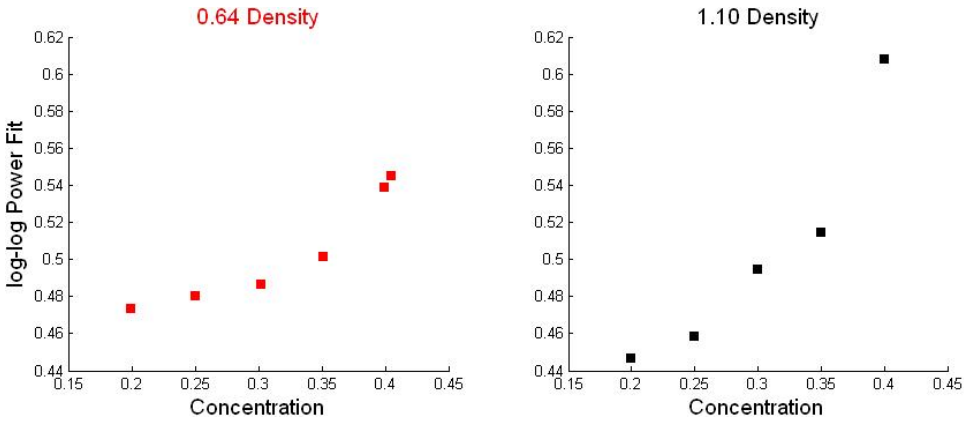

Figure 7: The calculated average exponential dependence at various concentrations for 2 particle densities

dence close to $t^{0.61}$, on average. We performed a baseline experiment in which we tested a clear fluid run. This proved to validate our method since the power fit was determined to be 0.34, which is very close to Huppert's $t^{1/3}$.

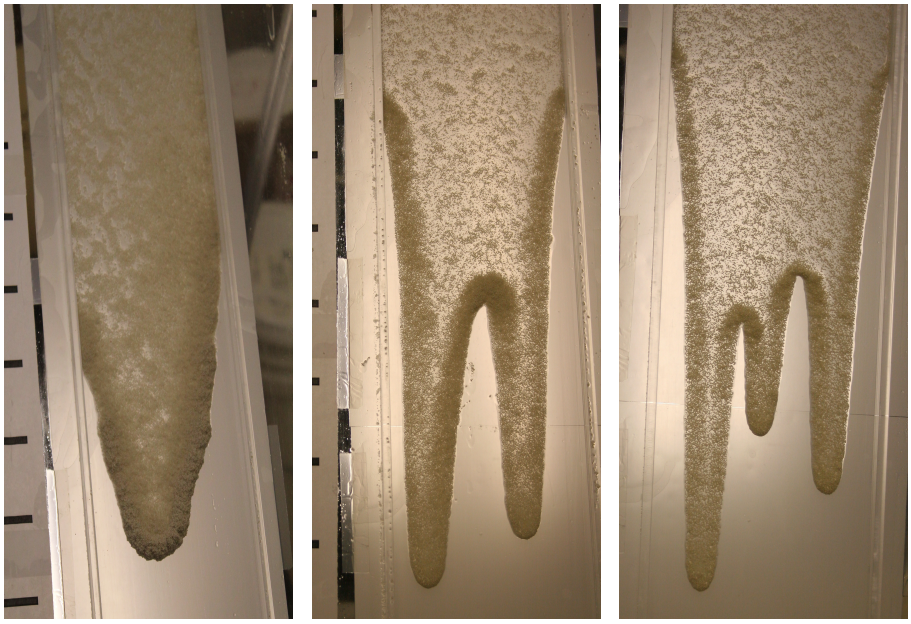

(a) 0.45 Concentration (b) 0.25 Concentration (c) 0.20 Concentration

Figure 8: Example fingering patters for particles of density 0.46 g/cm^3

In addition to the front tracking, we also analyzed each flow qualitatively by looking at the number of fingers which develop. For most flows, we see one, two, or three fingers (Figure 8); yet, in extreme cases, we may see four or more. The data we acquired seems to show that the number of fingers depends greatly upon the initial concentration of the mixture. Experiments at lower concentrations have a higher number of fingers, on average. With higher concentrations, the particles form a more concentrated ridge at the front which seems to suppress fingering for the most part. As our ϕ_0 approaches max packing, the number of fingers falls to one for each particle density (Figure 9).

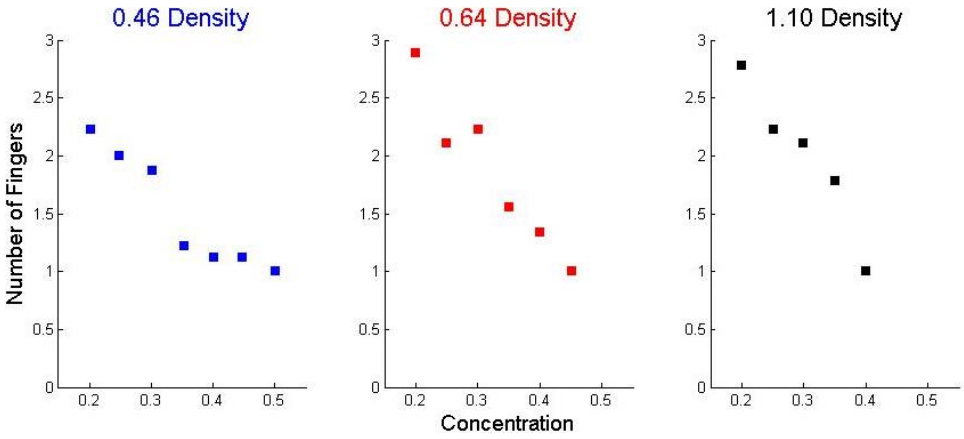

Figure 9: For each particle density, a plot is created to show the relation between concentration and the number of fingers present at the end of the run. At higher concentrations, fingering is suppressed.

4 Model Results

4.1 Cook PDE Model Derivation

4.1.1 Derivation

Cook developed a dynamic PDE model for heavy particle flows that exhibit the ridged regime. Using lubrication theory, it solves for vertically averaged particle concentration, ϕ, and total column particle volume, ϕh, at each point along the length of the flow. It is a system of two coupled equations that can be solved numerically using an upwind, finite differencing numerical scheme. Simple division enables extraction of film height h at each timestep.

4.1.2 Front Tracking

Cook's reduced dynamic model was used not only for qualitative comparison of experimental observations, but also to compare to Huppert's model of fluid front position with respect to time. Huppert [5] claims that the front position follows the equation 10 ($\hat{x_N} = (\frac{\hat{t}}{\hat{C_N}})^{1/3}$).

The front position was tracked and plotted as a function of $t^{1/3}$, revealing similar solutions as the experimental data. The simulations followed linear behavior in log-log plots as well as indicating an increasing power law as concentration became more diffuse. Figures show linear relationships in both power law fitting and as $t^{1/3}$.

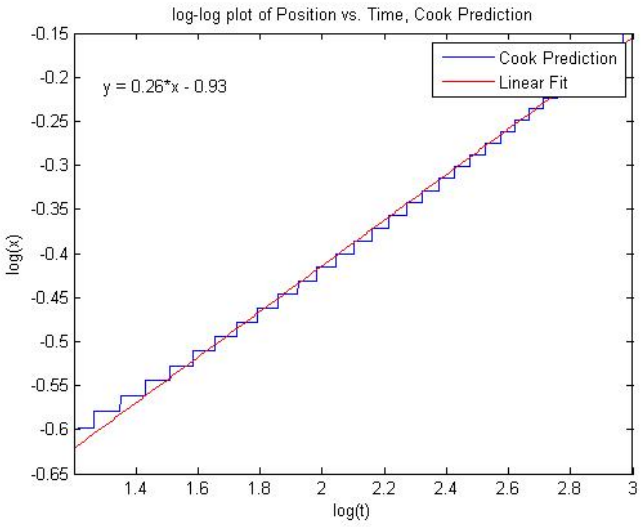

Figure 10: A log-log plot simulation of front position vs. time using the Cook model. Results are fairly linear with a power law fitting of 0.26.

The power fits predicted by the Cook model are close to Huppert's answer of 1/3, but is less than this value. For simulations of large diameter particle suspensions (density $0.46 g/cm^3$) in concentrations ranging from 0.05 to 0.50, in 0.05 increments, we found power law values decreasing with increasing concentrations, deviating from the expected value of 1/3. The details are summarized in Figure 12

The result of decreasing power fit with increasing concentration is a very in-

[5] [Huppert HE (1982) Flow and instability of a viscous current down a slope. Nature 300: 427429

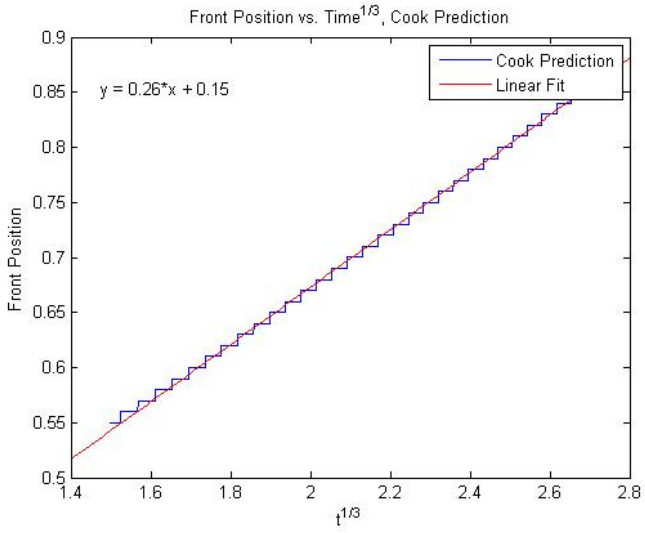

Figure 11: Position vs. $t^{1/3}$ is linear, for 0.45 concentration yielding a Huppert coefficient of 0.26.

Concentration	Power	Coefficient
0.05	0.28	0.55
0.10	0.28	0.52
0.15	0.27	0.48
0.20	0.27	0.45
0.25	0.27	0.40
0.30	0.27	0.36
0.35	0.28	0.32
0.40	0.28	0.27
0.45	0.26	0.21
0.50	0.22	0.12

Figure 12: Exponents and coefficients for different concentrations of Cook-simulated large particle suspension (particle density is $0.46 g/cm^3$) front positions. The power law fittings, while approaching 1/3 as less concentrated solutions are simulated, do not reach Huppert's value.

teresting result when compared to experiments. Empirical data shows that all power fits are larger than 1/3 and that as concentration increases, so does the power fit. While a comprehensive theory for the front position dynamics needs to be investigated, both numerical and empirical data for particle-laden suspensions suggest a departure from Huppert's model.

4.2 Steady-State ODE Model

Murisic et al. developed a first order ODE model for describing the equilibrium state of a thin-film PLF. This model includes shear-induced migration and hindered gravitational settling terms. It is solved numerically using a shooting scheme and calculates equilibrium vertical profiles for particle concentration, shear, and flow velocity. For heavy particles, this model accurately predicts either the settled, well-mixed, or ridged regime, depending on the inputted initial particle concentration and inclination angle. For light particles, the model also agrees well experimental data. That is, for all inclination angles and initial concentrations, the model predicts the ridged regime. It also predicts a parabolic vertical velocity profile, which lends credence to the accuracy of the Huppert scaling for these flows. It should be noted that this agreement with experiments is, at this stage, only qualitative. It is possible that the predicted concentration and velocity profiles by the model agree quantitatively with the experiments; however, experimental data on local concentration and velocity does not yet exist.

5 Hindered Settling

An experimental study of the hindered settling function was attempted by pictorially determining average particle height in a liquid suspension. Our method used digital images and centroid tracking, based on binary object area, to determine average particle position in a viscous medium. However analysis of average front position was not successful in producing a monotonic plot of position versus time.

We started our analysis with the terminal velocity of a particle rising through a viscous medium:

$$v_s = \frac{2}{9}\frac{(\rho_l - \rho_p)ga^2}{\mu_l} \tag{12}$$

also known as the Stokes settling velocity. We empirically determined the rising of a glass bead (P1, density $0.46g/cm^3$) in a volume of silicon oil.

However, increasing the concentration of particles in a suspension increases the number of particle-particle interactions, thus hindering the speed of the particles as they traverse through the suspension. In Cook et al, they propose a multiplicative equation to describe the relative settling velocity of the form:

$$V = v_s f(\phi) w(h) \tag{13}$$

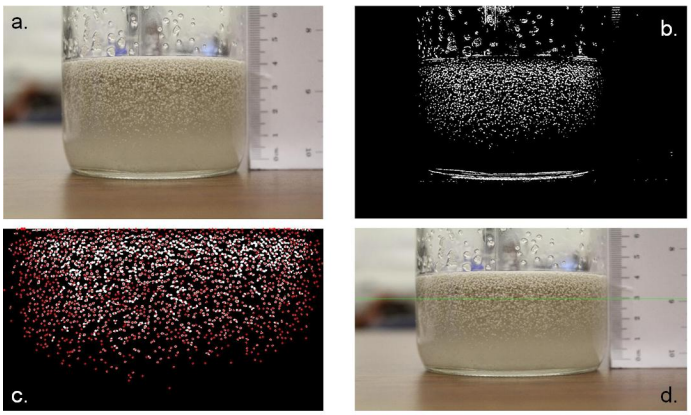

Figure 13: depicts the process of gathering image front position using the centroid tracking algorithm. In (a) the image is loaded into Matlab, (b) image is converted to binary, (c) the centroid of each object is found using Matlabs built-in commands. The centroid of the entire mass of particles is found by computing the center of mass of the system, (d) the average height is drawn and scaled using standardized measurement.

where f is the concentration dependent hindered settling function. While numerous studies have been done to empirically determine or theoretically derive such a function, Cook et al states that there is no comprehensive theory and we follow suit in their assumption that hindered settling and wall effects are multiplicative factors on the Stokes settling velocity. In our experiments we ignore wall effects assuming a function of the form:

$$V = v_s f(\phi) \tag{14}$$

where v_s is the settling velocity for a single particle. In our experiments we mixed concentrations ranging from 0.05 to 0.50 in intervals of 0.05, in 150mL batches. Suspensions were well-mixed by hand and particle migration was captured using a high-definition still shot camera with photo intervals approximately every 30 seconds (actual times obtained via a digital time stamp). A ruler is placed next to the fluid container and captured on camera as well. Photos were then processed in Matlab by cropping the photo into the region of interest, converting the image to binary, and finding the centroid of the mass of particles being viewed. The height of the centroid is then displayed and compared to the ruler in the shot for proper measurement.

We suspect the most crucial flaw in using image processing to obtain an average particle height is that still photos do not allow one to capture par-

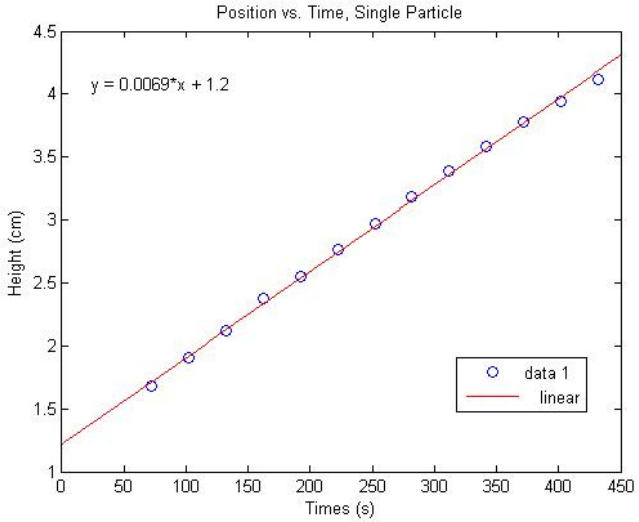

(a)

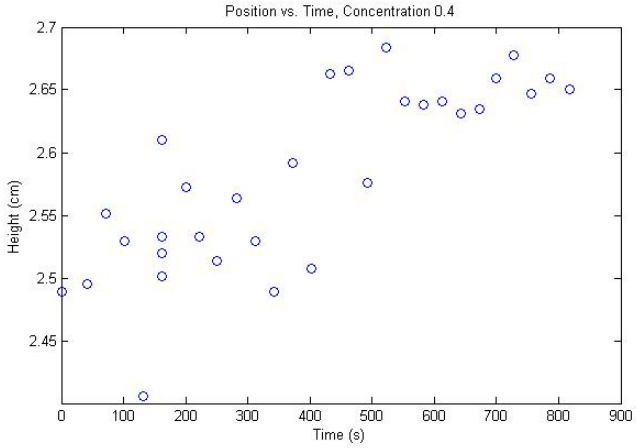

(b)

Figure 14: shows particle height position as it changes with time. (a): Experimental data for a single particle rising through a viscous medium. Height data was extracted using pixel counting and comparing to physical measurements. It follows a linear regression as predicted by classical mechanics. (b): Experimental data collected for a suspension of particles at and using the centroid tracking algorithm. While a general increase in height is observed, the data is not monotonic and cannot be properly fitted

ticles at a certain spatial depth in the liquid. Photographs only allow one to see particles closest to the wall of the container. We assumed that par-

ticle concentrations would be uniform over any differential horizontal layer. However in the conversion to binary, there is a non-uniform loss of particle mass at different layers in the fluid. Additionally, particles trail dust into the liquid solution making the fluid opaque and making it more difficult for Matlab to differentiate particles at a certain spatial depth with the surrounding liquid.

6 Conclusion

6.1 Key Findings

For particles of lower density than the suspending fluid, particles are transported to the front of the flow, thereby creating a particle-rich ridged flow front, for all inclination angles and concentrations. Although this is a significant deviation from flows with heavy particles, which can develop into one of three different regimes, it is not at all unexpected. This is because, in the light particle case, both the particle's buoyancy and shear-induced migration forces act in the same direction pushing particles towards the top of the flow, whereas in the heavy particle case these forces oppose one another. Though for heavy particles ridging tends to suppress fingering, fingers do develop for light particle flows, and their number is shown, on average, to decrease with increasing particle concentration. Nevertheless, models originally developed for heavy particle flows agree well with our experimental data on light particle flows. This fact suggests that the current theoretical description of PLFs is fairly robust, valid for both positively and negatively buoyant particles. More specifically, the reduced 1st order Cook dynamic PDE model accurately predicts a particle-rich ridged front whose speed roughly follows Huppert's $x = Ct^{1/3}$ scaling. The Murisic et al. steady-state ODE accurately predicts ridging for light particle flows of all concentrations and inclination angles. Arguably, it is not entirely surprising that the models developed originally for heavy particles extend to the light particle case well. All other experimental parameters held fixed, the fundamental difference between a light and heavy particle flow is the direction of the buoyant force, which the models take into account, provided that the sign of the Stokes settling velocity is adjusted as required by the physics.

6.2 Future Work

Due in part to delays in obtaining the light particles necessary to conduct experiments, data collection and image processing of the experimental runs

were not completed until near the end of the program. As such, analysis of the quantitative experimental data is still in its preliminary stage. Much more in-depth analysis of the data and comparison to the models – specifically working towards quantitative comparisons as much as possible – needs to be done.

Matthew Mata's 2D model of PLFs can be applied to light particle flows. This model is run in a moving reference frame and is for constant flux flows. Using a 2D model enables the simulation of fingering instabilities. This is quite useful, given that a majority of the light-particle flow experimental runs we conducted developed multiple fingers. A preliminary simulation of a two-finger flow agrees well qualitatively with experimental runs that developed two fingers. Specifically, the model predicts maximum particle concentration at the finger fronts. However, some runs with two fingers also had local concentration maximums at the splitting point at which the two fingers split, which the initial simulation does not show. Also, most fingers tend to be much longer down the track than the model simulated fingers.

Another tool for understanding the fingering instabilities is a linear stability analysis of the full 4th order Cook PDE model. Aliki Mavromoustaki has written some preliminary code that will enable this analysis. However, it is still in the debugging phase, and little data from this analysis is currently available.

In addition to the equilibrium ODE model, Murisic et al. also developed a dynamic PDE model that uses the ODE model to calculate particle concentration at each point both vertically and along the length of the track as the flow advances in time. This model was shown to qualitatively agree well with experimental results for heavy particles. Matthew Mata has begun coding up this model to apply it to the light particle case. However, this code is also still in the debugging phase and no model data is available as of yet.

Future experimental work could include an improved attempt at the empirical hindered "rising" function, collecting local concentration data, and using a laser sheet to determine the flow's shape for comparison to, for example, the Cook dynamic PDE model.

Empirically determining a hindered settling function was unsuccessful, however has given us insight into the technical needs of properly collecting data. We propose that three-dimensional data capture, possibly with the use of magnetic resonance imaging, will be more successful in arriving at a proper

hindered settling function.

6.2.1 Ridge Sampling

The concentration of particles at the front of a ridged regime flow is often assumed to be at the maximum packing density when modeling particle-laden slurry flow. This assumption is a major component in explaining and predicting the behavior of the flow in this regime. Among other behaviors large volume fraction of particles at the front when a ridge exists is used to explain the suppression of the fingering instability resulting in fewer fingers. As well as having significance for explaining the geometry of front flow for ridged flow it is known that when the concentration of particles reach maximum packing the flow at that point ceases to act as a fluid and begins to act as a solid leading to ridge break-off. While papers make the assumption that in the ridged regime at the free surface the particle concentration is close to the maximum packing (slightly smaller since solid-like behavior is not modeled) no measurement is made of the local particle volume fraction. We made a successful attempt to measure the ridge particle concentration for particles of a greater density than the liquid.

The method found to be successful for finding the ratio of particles (p) to liquid (l) in the ridge relied upon an ability to accurately measure the volume, V, and mass, m, of a ridge sample. When a run resulted in a pronounced ridge a sample was scraped off the track and deposited into a graduated cylinder. The graduated cylinder is prepared by filling it to a known volume with water or preferably a liquid that is less dense than the liquid in the slurry on the track. The filled cylinder is massed on a scale such that the difference in the mass before and after the sample is added can be used to determine the mass of the sample. the change in the level of the liquid in the graduated cylinder can be used to find the volume of the sample. The concentration may then be found using the following coupled equations.

$$m_T = m_p + m_l \tag{15}$$

$$V_t = V_p + V_l = \rho_p \cdot m_p + \rho_p \cdot m_l \tag{16}$$

By combining these equations it is possible to find the mass of both components leading to the concentration of the ridge.